Synthesis and Characterization of Organic–Inorganic Hybrid GeOx/Ethylenediamine Nanowires

ARTICLE *in* ADVANCED MATERIALS · MAY 2008

Impact Factor: 17.49 · DOI: 10.1002/adma.200701646

4 AUTHORS, INCLUDING:

Qingsheng Gao
Jinan University (Guangzhou, China)
25 PUBLICATIONS **632** CITATIONS
SEE PROFILE

Yi Tang
Fudan University
120 PUBLICATIONS **2,812** CITATIONS
SEE PROFILE

DOI: 10.1002/adma.200701646

Synthesis and Characterization of Organic–Inorganic Hybrid GeO_x/Ethylenediamine Nanowires**

By *Qingsheng Gao, Ping Chen, Yahong Zhang,** and *Yi Tang**

The promising research on organic–inorganic hybrid materials (including their synthesis, characterization, and modification) has attracted extensive interest because of their unique properties and potential applications in various fields including catalysis, sensing technology, optoelectronics, and electromagnetics.[1] In the past decade, several kinds of organic–inorganic hybrid particles of micrometer size have been synthesized, such as $MQ(L)_x$ (M = Mn, Zn, Cd; Q = S, Se, Te; L = mono- or diamine or hydrazine; $x = 0.5$ or 1.0).[2] They were believed to combine the superior features of both inorganic frameworks and organic components, thus improving their functionality and performance.[1c,3] Significantly, the sub-nanometer-scale periodic structures in these hybrid materials led to strong quantum confinement effects (QCEs), which are important for achieving suitable bandgaps in order to design functional devices.[2d,3b,4] In addition,1D nanostructures have become a highlight in materials science and recently remarkable progress has been achieved for the preparation of 1D organic–inorganic hybrid nanocrystals, e. g., ZnS/N_2H_4,[5a] ZnS/cyclohexylamine,[5b] $WO_{2.72}(N_6C_{123}H_{136}O_{22})_{0.04}$,[5c,5d] ZnS/n-butylamine nanowires,[5e] and ZnSe(diethylenetriamine)$_{0.5}$ nanobelts.[5f] Besides the prominent properties of 1D nanostructures, the strong QCEs resulting from the sub-nanometer dimensions could tune the electronic and optical properties.[5a,5b,5e,5f] Therefore, the preparation of sub-nanometer-scale periodic organic–inorganic hybrid structures that can be integrated with 1D nanocrystals will undoubtedly lead to 1D nanomaterials that can be applied as functional segments or building blocks in various nanodevices.

1D GeO_2 nanomaterials are considered as potentially important functional components and interconnections in future optoelectronic nanodevices,[6a,6b] because GeO_2 nanocrystals are blue photoluminescence materials[6c] and GeO_2-based glass is thought to be more refractive than its corresponding silicate.[6b] A series of functional materials with strong QCEs and tunable optical properties is expected to be obtained when sub-nanometer-scale periodic hybrid structures are integrated into 1D nanoscaled GeO_2. However, to our knowledge, such structures cannot be achieved with current strategies.

In this Communication, novel organic–inorganic hybrid GeO_x/EDA (EDA = ethylenediamine) nanowires with a sub-nanometer periodic structure are fabricated in a high yield via an Fe_2O_3-assisted liquid-phase hydrothermal method. An Fe_2O_3-assisted mechanism is proposed for the anisotropic growth of the hybrid nanowires. This provides opportunites for the development of new nanomaterials for future applications in electromagnetics, optoelectronics, and sensing technology. The synthesis of GeO_x/EDA nanowires was carried out by directly mixing GeO_2 with Fe_2O_3 and then treating the mixture in an aqueous EDA solution at 200 °C for 5 days. Unlike the previously reported method,[7] this aqueous-phase procedure is more convenient and has potential for large-scale manufacturing. A typical scanning electron microscopy (SEM) image (Fig. 1a) shows that the as-obtained product possesses a uniform, wirelike morphology with a diameter of 50 ~ 120 nm and a length of several tens of micrometers. The transmission electron microscopy (TEM, Fig. 1b) image shows a clearly visible set of periodic black/white strips occuring across the whole nanowire; the period was ~ 1.10 nm wide. Correspondingly, the X-ray diffraction (XRD) pattern displays an intensive diffraction peak at $2\theta = 7.93°$ (i.e., $d = 1.113$ nm, Fig. 1c). Comparison with the powder-diffraction file (PDF)-database of the International Centre for Diffraction Data (ICDD) and calculations performed with the MDI/JADE 6.0 program (see Table S1 of the Supporting Information) revealed that the GeO_x/EDA nanowires exhibited a new crystalline structure in a monoclinic system with space group *Cc*9; the unit-cell parameters were $a = 19.632$ Å, $b = 14.038$ Å, $c = 5.932$ Å, and $\beta = 110.7°$. The structure was further validated by measuring a selected-area electron diffraction (SAED) pattern (Fig. 1d), which was well indexed in comparison to the results of the simulated XRD pattern. In the corresponding TEM image (magnification 4×10^5, Fig. 1e), the *d*-spacings of 1.10 and 0.44 nm were clearly observed, which were indexed as (110) and $(22\bar{1})$, respectively. These were confirmed by inverse fast Fourier transformation (IFFT, Fig. 1f). In addition, a single nanowire was viewed along another zone axis, $[0\bar{2}2]$, showing that the *d*-spacings and interplane angles were consistent with the simulated results (see Fig. S1 in the Supporting Information).

Energy-dispersive spectroscopy (EDS, Fig. 2a) and electron energy-loss spectra (EELS, see Fig. S2 of the Supporting

[*] Dr. Y. H. Zhang, Prof. Y. Tang, Q. S. Gao, P. Chen
Department of Chemistry
Shanghai Key Laboratory of Molecular Catalysis and Innovative Materials and Laboratory of Advanced Materials
Fudan University
Shanghai 200433 (P.R. China)
E-mail: yitang@fudan.edu.cn; zhangyh@fudan.edu.cn

[**] This work is supported by the NSFC (20325313, 20673026, 20721063), the STCSM (06DJ14006) and Major State Basic Research Development Program (2003CB615807). We thank Prof. C. Z. Yu for assistance with the EFTEM and EELS characterization and Prof. G. L. Lü for assistance with the XRD characterization. Supporting Information is available online from Wiley Interscience or from the author.

ADVANCED MATERIALS

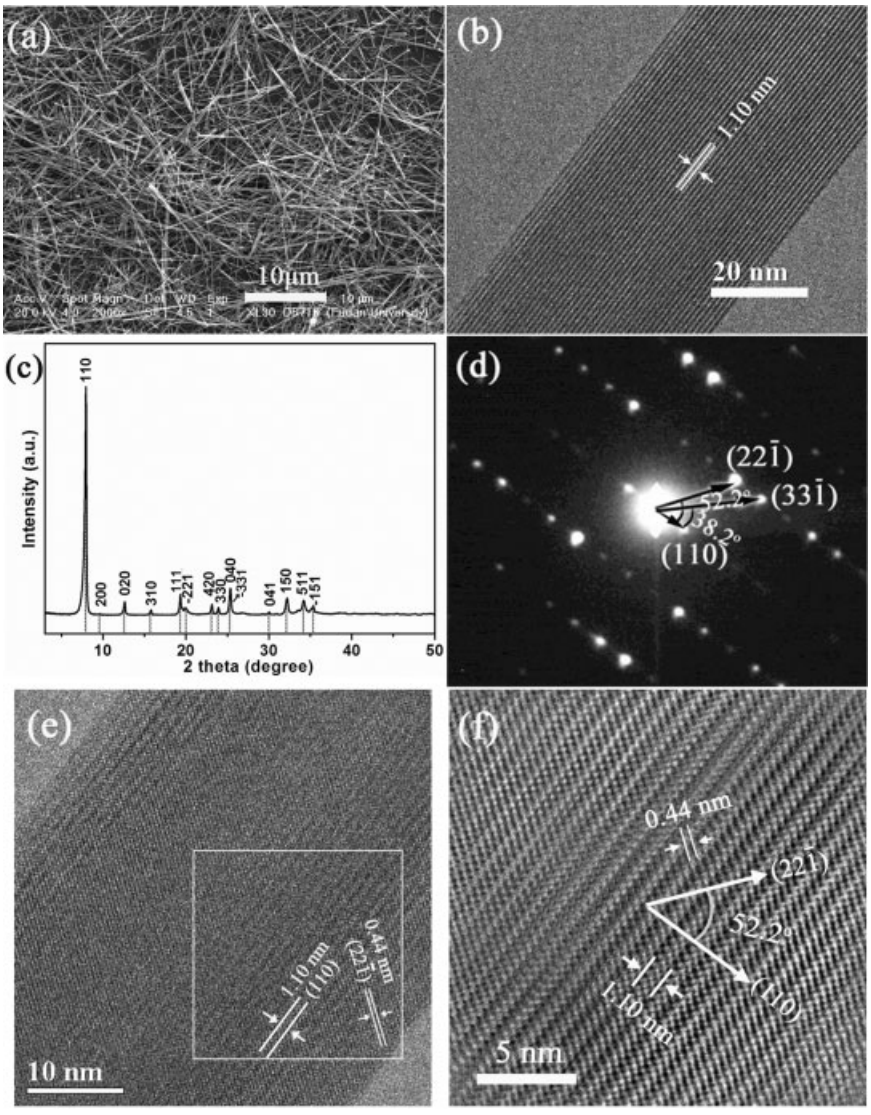

Figure 1. a) SEM image, b) TEM image, and c) XRD pattern of the as-synthesized nanowires. d) SAED pattern and e) high-magnification TEM image of the nanowire shown in (b). f) IFFT of the square region in (e).

Information) were used to determine the composition of a single nanowire; only the signals of Ge, O, C, and N were identified in the nanowire. Furthermore, nitrogen mapping (Fig. 2b) obtained by energy-filtering TEM (EFTEM) equipped with EELS suggested a uniform nitrogen distribution in the body of the nanowire, meaning that EDA intercalates uniformly in the structure. The presence of EDA was confirmed by the characteristic absorption peaks in the IR spectrum of GeO_x/EDA nanowires (Fig. 3a); EDA-assigned peaks included the stretching vibrations of $-NH_2$ (3336 and 3287 cm^{-1}), $-CH_2$ (2948 and 2878 cm^{-1}), C–N (1023 cm^{-1}), and the in-plane (1592 cm^{-1}) and out-plane (847 and 803 cm^{-1}) bending vibrations of $-NH_2$.[8]

After calcination in an air flow at 600 °C for 5 h, the morphology of nanowires was still intact (see Fig. S3a of the Supporting Information); however, the original pattern of black/white strips (cf. Fig. 1b) had vanished (see Fig. S3b of the Supporting Information). Correspondingly, the diffraction peak at $2\theta = 7.93°$ (cf. Fig. 1c) also disappeared after calcination and the XRD pattern reverted to that of the inorganic α-GeO_2 phase (see Fig. S3c of the Supporting Information). Additionally, when 1,6-hexanediamine (possessing a longer carbon-skeleton) was employed instead of EDA during the preparation, nanowires with wider periodic black/white strips (~1.40 nm) could be obtained (see Fig. S4 of the Supporting Information). It was concluded that the

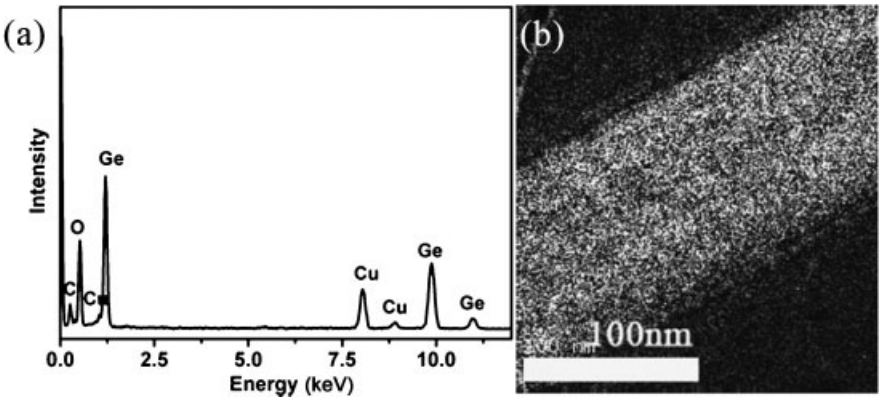

Figure 2. a) EDS and b) nitrogen-mapping image of a single as-synthesized nanowire. The nitrogen-mapping image was obtained with EFTEM equipped with EELS.

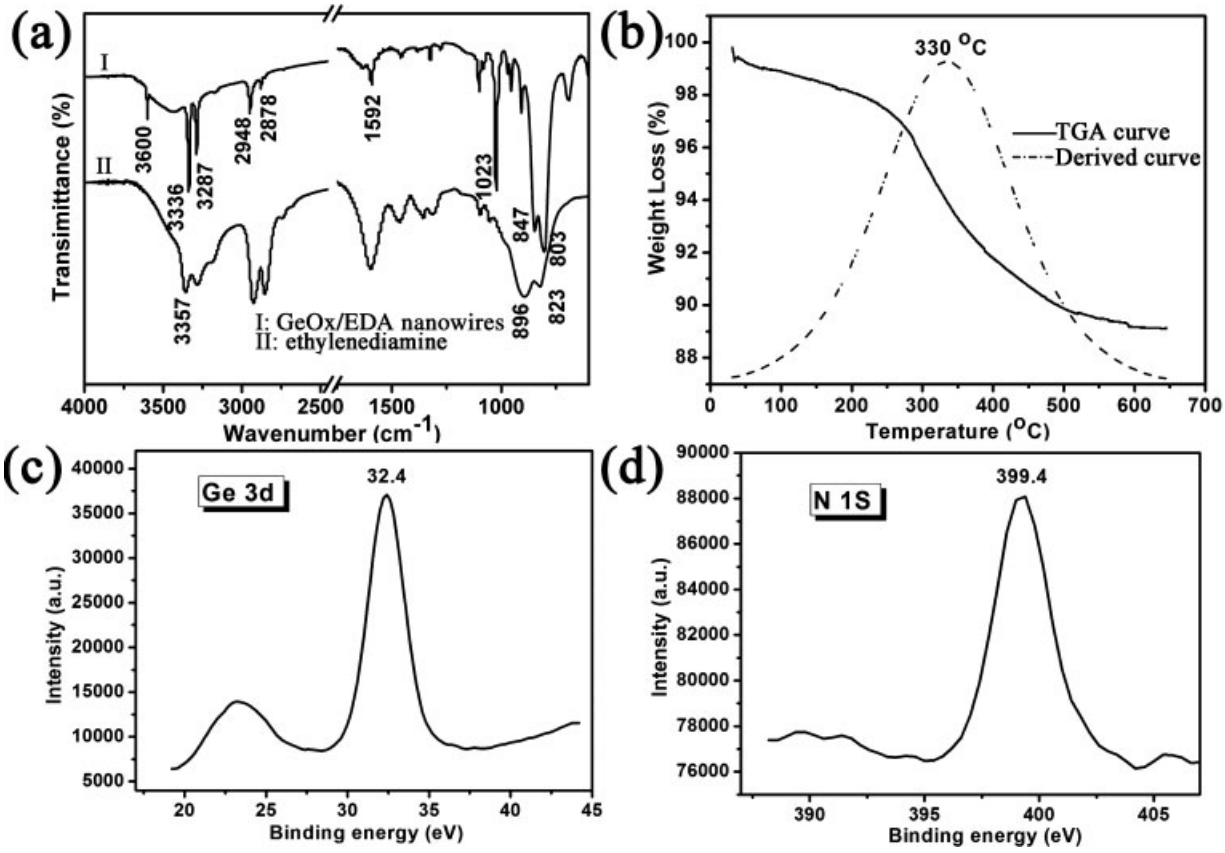

Figure 3. a) IR spectra of the GeO_x/EDA nanowires (I) and EDA (II), b) TGA, c) Ge 3d XPS and d) N 1s XPS of the GeO_x/EDA nanowires.

subnanometer-scale striate structure in the GeO_x/EDA nanowires originated from the intercalation of the diamine.

Thermogravimetric analysis (TGA) and X-ray photoelectron spectroscopy (XPS) were used in combination with IR spectroscopy to investigate the structure of the hybrid nanowires in more detail. The TGA plot of the GeO_x/EDA nanowires (Fig. 3b) displays a large weight loss at 330 °C, which was attributed to the evaporation or decomposition of EDA. The weight loss occurred at temperatures above the EDA boiling point (117 °C) indicating that an interaction existed between EDA and the inorganic framework,[9] rendering the removal of EDA difficult. This interaction was further confirmed by a red-shift of the absorption peaks of the nanowires (Fig. 3a) assigned to the stretching and out-plane bending vibration of $-NH_2$[9] when compared to the absorption peaks of EDA, which showed molecular stretching at 3357 cm^{-1} and bending at 896 and 823 cm^{-1}. However, XPS measurements (Fig. 3c) showed that the Ge 3d binding energy (32.4 eV) of the hybrid nanowires was almost identical to that of Ge (IV) (32.5 eV) in GeO_2,[10] meaning that the interaction was weak. Considering that the IR spectrum did not contain a broad peak of protonated alkylamines at $3000 \sim 2500\ cm^{-1}$[8] (Fig. 3a) and that the binding-energy value of N 1s in the nanowires (399.4 eV, Fig. 3d) is close to the binding-energy value of alkylamine (399.6 eV), but not to that (402.4 eV) of alkylammonium,[11] it can be assumed that the EDA intercalated in the nanowires is not in the form $-NH_3^+$. Additionally, the IR spectrum of GeO_x/EDA also displays a narrow absorption peak at 3600 cm^{-1}, suggesting an abundant presence of –OH in the hybrid nanowires.[8] Therefore, the weak interaction between EDA and the inorganic framework can be ascribed to the (N–H•••O–Ge) H-bonding, which resembles the relatively weak (N–H•••O–P) H-bonding resulting from alkylamines intercalating into the structure of α-$Zr(HPO_4)_2 \bullet H_2O$.[12] Therefore, on basis of these results, a model (Scheme 1) is proposed for the hybrid nanowires: the EDA intercalating into the nanowires connects the sub-nanometer inorganic units through (N–H•••O–Ge) H-bonding to achieve the organic–inorganic hybrid structure, which is similar to the metal–chalcogen layers pillared by amine in ZnS/cyclohexylamine nanowires.[5b]

The room-temperature UV/vis spectra depicted in Figure 4 were measured with samples that were predispersed well in ethanol by means of ultrasonic treatment. The curve of the GeO_x/EDA nanowires exhibits an obvious blue-shift ($\Delta\lambda = 9$ nm) from 252 to 243 nm in comparison to those of commercial α-GeO_2 powder and α-GeO_2 nanowires obtained after calcining the hybrid nanowires at 600 °C (Fig. 4). This phenomenon could be explained by the QCE resulting from the sub-nanometer periodic structure.[2c] With its large

ADVANCED MATERIALS

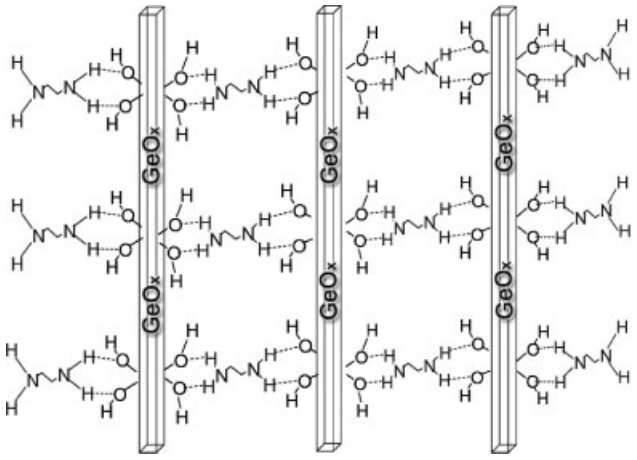

Scheme 1. Schematic representation of the structure of organic–inorganic hybrid GeO_x/EDA nanowires.

bandgap (5.95 eV, corresponding to the UV absorption at 209 nm in Fig. S5 of the Supporting Information), the EDA molecule acts as a barrier and causes the strong quantum confinement of both electrons and holes in the inorganic region, similar to the case of $ZnTe(EDA)_{0.5}$.[4] The organic–inorganic hybrid structure considerably changed the optical-absorption edge of GeO_2 for the QCE, which might provide a new approach to modulate the optical properties of 1D germanium oxide nanostructures. Furthermore, the bright blue light emitted by the GeO_x/EDA nanowires with a peak at 425 nm (excited at 400 nm) could clearly be observed using confocal fluorescence microscopy (see Fig. S6 of the Supporting Information), suggesting potential applications of hybrid nanowires in future integrated optical nanodevices.[13]

Based on the experimental results, we have confirmed that EDA intercalates into the inorganic GeO_x framework to form novel hybrid nanowires with a sub-nanometer-scaled period. The inorganic units are connected by EDA via H-bonding of (N–H•••O–Ge). It has been reported that coordination between an alkylamine and metal cations may induce anisotropic growth of nanowires in a system containing elements of the groups *II* and *VI*, which was termed as the solvent-coordination molecular-template (SCMT) mechanism.[14] However, in our experiments, only bulky products were obtained from the hydrothermal system without Fe_2O_3, or from a vapor-phase hydrothermal process in which GeO_2 powder was separated from Fe_2O_3 (see Fig. S7 of the Supporting Information). These observations imply that another mechanism—taking into account a direct assisted effect from Fe_2O_3 may underlie the growth of the GeO_x/EDA nanowires. To confirm the occurrence of the assisted effect of Fe_2O_3 for the formation of GeO_x/EDA nanowires, a surface-oxidated iron sheet was employed to replace Fe_2O_3. Uniform nanowires were obtained on the surface of the sheet, while a predominantly bulky product was formed away from the sheet (see Fig. S8 of the Supporting Information), proving that direct contact between Fe_2O_3 and GeO_2 is indispensable for the growth of the nanowires. Therefore, a Fe_2O_3-assisted mechanism is proposed for the growth of GeO_x/EDA nanowires (Scheme 2). First, EDA is enriched on the surface of Fe_2O_3 for the coordination between EDA and $Fe^{\delta+}$ ($\delta < 3$). Due to the weak oxidative ability of Fe(III) in an alkaline solution, the lone pair of electrons on the nitrogen atoms transfers to $Fe^{\delta+}$, and simultaneously the oxygen atoms in $Ge(OH)_4$, derived from the dissolution of GeO_2, associate with the hydrogen atoms in $-NH_2$ due to the oxidation tendency of EDA,[15] which promotes the formation of (N–H•••O–Ge) H-bonding. Then, neighboring Ge–OH bonds begin to condense under hydrothermal conditions at 200 °C, producing primary organic–inorganic hybrid units on the Fe_2O_3 surface. The primary units formed with EDA attached in-plane via (N–H•••O–Ge) H-bonding will be expelled as other EDA molecules attack the $Fe^{\delta+}$. The attached EDA would hinder the in-plane growth of the inorganic unit, resulting in anisotropic growth in the vertical direction. Such growth induced by attached EDA molecules is analogous to the SCMT mechanism for the growth of 1D metal chalcogenide[14] and $Mg(OH)_2$.[16] Furthermore, these ultrathin units are not stable because of their high surface energy under hydrothermal conditions at 200 °C, and tend to assemble with each other along the in-plane direction. Therefore, the hybrid nanowires are generated through anisotropic growth induced by EDA and direct assistance of the Fe_2O_3 surface.

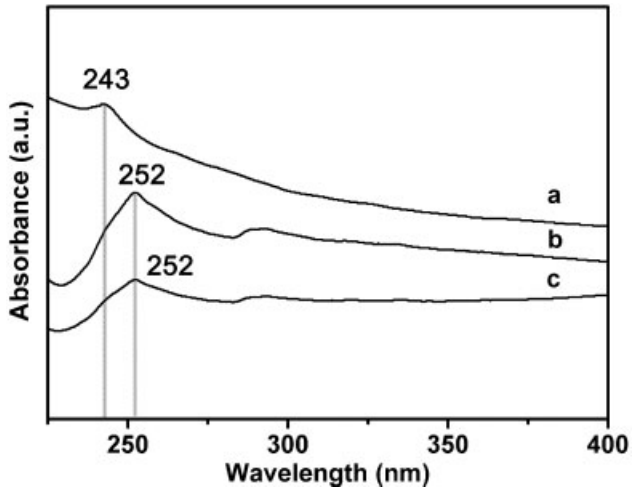

Figure 4. UV/vis spectra of a) GeO_x/EDA hybrid nanowires, b) α-GeO_2 nanowires and c) α-GeO_2 powder.

In summary, novel organic–inorganic hybrid GeO_x/EDA nanowires were synthesized via a Fe_2O_3-assisted liquid-phase hydrothermal method. The structure is a monoclinic system with space group *Cc*9 and the unit cell parameters are: $a = 19.632$ Å, $b = 14.038$ Å, $c = 5.932$ Å, and $\beta = 110.7°$. EDA connects the inorganic units through (N–H•••O–Ge) H-bonding to form a unique organic–inorganic hybrid sub-nanometer periodic structure, which exhibits an obvious QCE. A Fe_2O_3-assisted growth mechanism is proposed, in

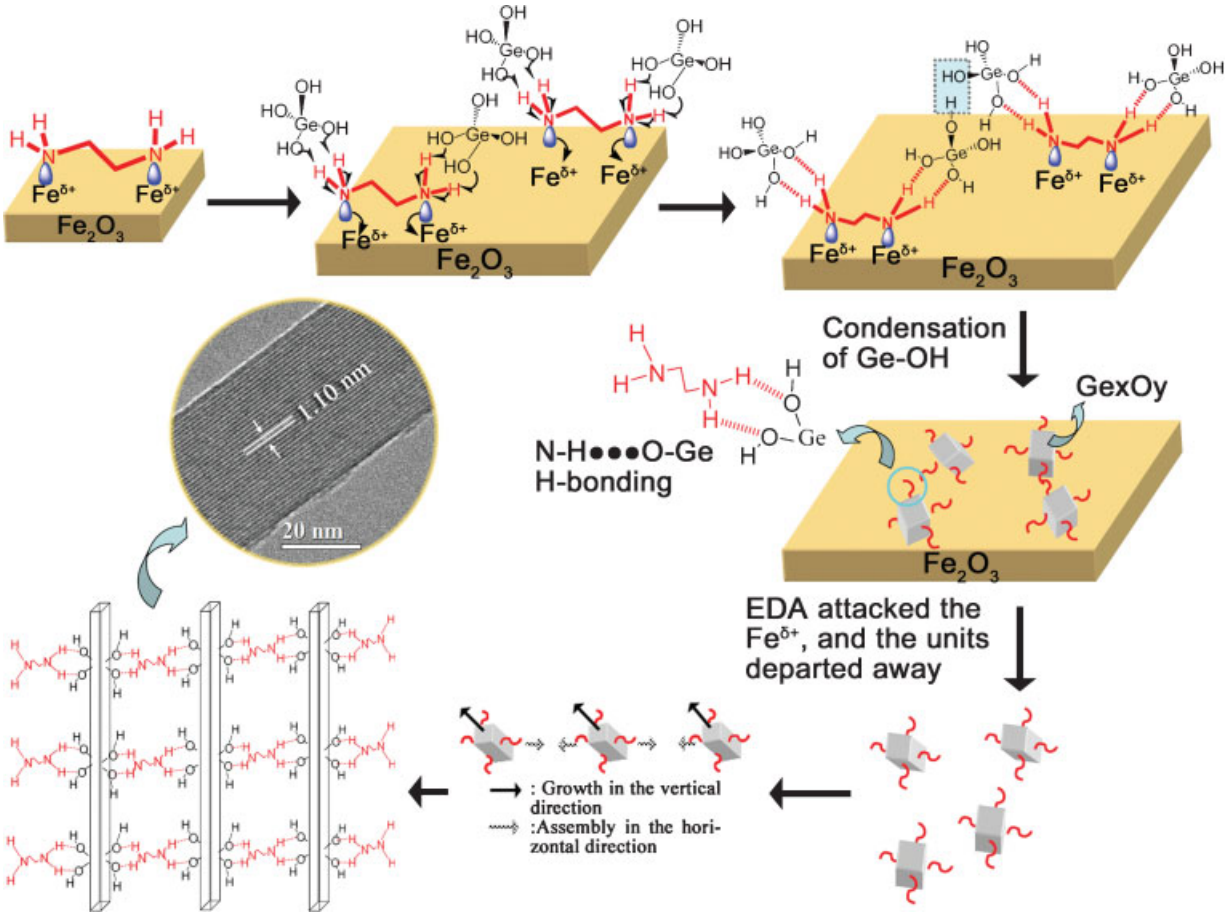

Scheme 2. Schematic representation of the growth mechanism of GeO_x/EDA hybrid nanowires.

which the H-bonding of (N–H•••O–Ge) generated by the direct assistance of Fe_2O_3 induces the anisotropic growth of these hybrid nanowires. Although further research is needed to establish the exact growth mechanism, the presented method will promote the preparation of other organic–inorganic hybrid 1D nanostructured materials, which display tunable electronic and optical properties that allow application in future functional nanodevices.

Experimental

In a typical procedure, 0.1 g GeO_2 was mixed with 0.05 g Fe_2O_3 by milling for several minutes. Then, the mixture was transferred to a Teflon-lined stainless-steel autoclave filled with 0.8 ml H_2O and 0.5 ml EDA. After hydrothermal treatment at 200 °C for 5 days, the product was collected after centrifugation, then three times thoroughly washed with ethanol, and finally dried at 75 °C. The synthesis of hybrid nanowires intercalated with 1,6-hexanediamine was carried out under the same conditions, except for replacing EDA by 1,6-hexanediamine and changing the volume of diamine to 0.8 ml.

XRD patterns were taken on a Rigaku D/MAX PC2550 diffractometer using Cu Kα radiation ($\lambda = 1.54056$ Å). TEM and SEM images were obtained on a JEOL JEM-2010 and a Philips XL 30, respectively. EFTEM and EELS measurements were carried out on a Philips Tecnai G2 F30 TEM. IR spectroscopy investigations were performed on a Nicolet 360 FT-IR spectrometer. TGA was carried out on a Perkin-Elmer TGA7. XPS measurements were performed on a Perkin-Elmer PHI5000c XPS, using C 1s (B. E. = 284.6 eV) as a reference. UV/vis spectra were obtained with a Shimadzu UV-2045 PC at room temperature; the samples had been predispersed well in ethanol by ultrasonic treatment. Micro-photoluminescence spectra and confocal fluorescence microscopy images were taken on a Princeton Instruments SP2150i with a charge-coupled device (CCD) spectrometer (Princeton Instruments 7508-0001).

Received: July 10, 2007
Revised: January 17, 2008
Published online: April 17, 2008

[1] a) T. Asefa, M. J. MacLachlan, N. Coombs, G. A. Ozin, *Nature* **1999**, *402*, 867. b) S. R. Batten, R. Robson, *Angew. Chem. Int. Ed.* **1998**, *37*, 1460. c) S. Coe, W. K. Woo, M. Bawendi, V. Bulovic, *Nature* **2002**, *420*, 800. d) K. Yamamoto, Y. Sakata, Y. Nohara, Y. Takahashi, T. Tatsumi, *Science* **2003**, *300*, 470. e) S. Park, S. W. Chung, C. A. Mirkin, *J. Am. Chem. Soc.* **2004**, *126*, 11772.

[2] a) S. H. Yu, M. Yoshimura, *Adv. Mater.* **2002**, *14*, 296. b) X. Y. Huang, J. Li, H. X. Fu, *J. Am. Chem. Soc.* **2000**, *122*, 8789. c) X. Y. Huang, H. R. Heulings, IV, V. Le, J. Li, *Chem. Mater.* **2001**, *13*, 3754. d) H. R. Heulings, IV, X. Y. Huang, J. Li, T. Yuen, C. L. Lin, *Nano. Lett.* **2001**, *1*, 521. e) Z. X. Deng, L. B. Li, Y. D. Li, *Inorg. Chem.* **2003**, *42*, 2331. f) X. Y. Huang, J. Li, Y. Zhang, A. Mascarenhas, *J. Am. Chem. Soc.*

2003, *125*, 7049. g) C. Y. Moon, G. M. Dalpian, Y. Zhang, S. H. Wei, X. Y. Huang, J. Li, *Chem. Mater.* **2006**, *18*, 2805. h) X. Y. Huang, J. Li, *J. Am. Chem. Soc.* **2007**, *129*, 3157.

[3] a) M. C. Lonergan, *Science* **1997**, *278*, 2103. b) B. Fluegel, Y. Zhang, A. Mascarenhas, X. Huang, J. Li, *Phys.* Rev. B **2004**, *70*, 205308.

[4] Y. Zhang, G. M. Dalpian, B. Fluegel, S. H. Wei, A. Mascarenhas, X. Y. Huang, J. Li, L. W. Wang, *Phys. Rev. Lett.* **2006**, *96*, 026405.

[5] a) Y. J. Dong, Q. Peng, Y. D. Li, *Inorg. Chem. Comm.* **2004**, *7*, 370. b) L. B. Fan, H. W. Song, H. F. Zhao, G. H. Pan, H. Q. Yu, X. Bai, S. W. Li, Y. Q. Lei, Q. L. Dai, R. F. Qin, T. Wang, B. Dong, Z. H. Zheng, Xinguang Ren, *J. Phys. Chem. B* **2006**, *110*, 12948. c) J. Polleux, N. Pinna, M. Antonietti, M. Niederberger, *J. Am. Chem. Soc.* **2005**, *127*, 15595. d) J. Polleux, A. Gurlo, N. Barsan, U. Weimar, M. Antonietti, M. Niederberger, *Angew. Chem. Int. Ed.* **2006**, *45*, 261. e) W. T. Yao, S. H. Yu, Q. S. Wu, *Adv. Funct. Mater.* **2007**, *17*, 623. f) W. T. Yao, S. H. Yu, X. Y. Huang, J. Jiang, L. Q. Zhao, L. Pan, J. Li, *Adv. Mater.* **2005**, *17*, 2799.

[6] a) Z. G. Bai, D. P. Yu, H. Z. Zhang, Y. Ding, Y. P. Wang, X. Z. Cai, Q. L. Hang, G. C. Xiong, S. Q. Feng, *Chem. Phys. Lett.* **1999**, *303*, 311. b) Y. Su, Z. Y. He, Y. Q. Chen, J. Jiang, D. Cai, L. Chen, *Mater. Lett.* **2005**, *59*, 2990. c) M. Zacharias, P. M. Fauchet, *J. Non-Cryst. Solids* **1998**, *227*, 1058.

[7] P. Chen, S. H. Xie, N. Ren, Y. H. Zhang, A. G. Dong, Y. Chen, Y. Tang, *J. Am. Chem. Soc.* **2006**, *128*, 1470.

[8] S. F. Dyke, H. J. Floyd, M. Sainsburg, R. S. Theobald, *Organic Spectroscopy An Introduction*, 2nd ed., Longman Inc., New York **1978**, *80.*

[9] Z. X. Deng, L. B. Li, Y. D. Li, *Inorg. Chem.* **2003**, *42*, 2331.

[10] N. Tabet, M. Faiz, N. M. Hamdan, Z. Hussain, *Surf. Sci.* **2003**, *523*, 68.

[11] a) B. J. Meldrum, C. H. Rochester, *J. Chem. Soc. Faraday Trans.* **1990**, *86*, 1881. b) R. J. J. Jansen, H. Van Bekum, *Carbon* **1995**, *33*, 1021.

[12] A. Clearfield, R. M. Tindwa, *J. Inorg. Nucl. Chem.* **1979**, *41*, 871.

[13] Z. Jiang, T. Xie, G. Z. Wang, X. Y. Yuan, C. H. Ye, W. P. Cai, G. W. Meng, G. H. Li, L. D. Zhang, *Mater. Lett.* **2005**, *59*, 416.

[14] a) Y. D. Li, H. W. Liao, Y. Ding, Y. Fan, Y. Zhang, Y. T. Qian, *Inorg. Chem.* **1999**, *38*, 1382. b) Y. D. Li, H. W. Liao, Y. Ding, Y. T. Qian, L. Yang, G. E. Zhou, *Chem. Mater.* **1998**, *10*, 2301.

[15] J. March, *Advanced Organic Chemistry (Reactions, Mechanisms, and Structure)*, 3rd ed., John Wiley & Sons Inc., New York **1985**, *1086.*

[16] Y. D. Li, M. Sui, Y. Ding, G. H. Zhang, J. Zhuang, C. Wang, *Adv. Mater.* **2000**, *12*, 818.

